Coaxial Electrospinning of (Fluorescein Isothiocyanate-Conjugated Bovine Serum Albumin)-Encapsulated Poly(ϵ-caprolactone) Nanofibers for Sustained Release

Y. Z. Zhang,*[,†,‡,§] X. Wang,[||] Y. Feng,[†] J. Li,[†,§,||] C. T. Lim,[†,‡,§] and S. Ramakrishna[†,‡,§]

Division of Bioengineering, Department of Mechanical Engineering, and Nanoscience and Nanotechnology Initiative, National University of Singapore, 9 Engineering Drive 1, Singapore 117576, and Institute of Materials Research and Engineering, 3 Research Link, Singapore 117602

Received October 5, 2005; Revised Manuscript Received February 8, 2006

As an aim toward developing biologically mimetic and functional nanofiber-based tissue engineering scaffolds, we demonstrated the encapsulation of a model protein, fluorescein isothiocyanate-conjugated bovine serum albumin (fitcBSA), along with a water-soluble polymer, poly(ethylene glycol) (PEG), within the biodegradable poly(ϵ-caprolactone) (PCL) nanofibers using a coaxial electrospinning technique. By variation of the inner flow rates from 0.2 to 0.6 mL/h with a constant outer flow rate of 1.8 mL/h, fitcBSA loadings of 0.85−2.17 mg/g of nanofibrous membranes were prepared. Variation of flow rates also resulted in increases of fiber sizes from ca. 270 nm to 380 nm. The encapsulation of fitcBSA/PEG within PCL was subsequently characterized by laser confocal scanning microscopy, transmission electron microscopy (TEM), and X-ray photoelectron spectroscopy (XPS) analysis. In vitro release studies were conducted to evaluate sustained release potential of the core−sheath-structured composite nanofiber PCL-r-fitcBSA/PEG. As a negative control, composite nanofiber PCL/fitcBSA/PEG blend was prepared from a normal electrospinning method. It was found that core−sheath nanofibers PCL-r-fitcBSA/PEG pronouncedly alleviated the initial burst release for higher protein loading and gave better sustainability compared to that of PCL/fitcBSA/PEG nanofibers. The present study would provide a basis for further design and optimization of processing conditions to control the nanostructure of core−sheath composite nanofibers and ultimately achieve desired release kinetics of bioactive proteins (e.g., growth factors) for practical tissue engineering applications.

1. Introduction

With the revival of the nanofiber manufacturing technology termed "electrospinning"[1−3] in the past few years, great efforts have been made to use polymeric nanofibers as scaffolding materials for engineering a variety of tissues. One advantage that these nanofibers have is that they can biologically mimic the physical structure of native extracellular matrix (ECM).[4−6] As the nanofibers are dimensionally small and physically weak, the nanofiber-based artificial scaffolds could be more effective for cells to remodel the cell-scaffold system toward better integrity and final regeneration of natural ECM as the scaffold materials degrade over time.

From the tissue engineering point of view, besides cells and scaffolds, another indispensable and important element is the growth factors, which should be delivered in a controlled and sustained manner without loss of its bioactivity. Many critical phenomena in tissue development, e.g., cell patterning, motility, proliferation, aggregation, and gene expression, are influenced by those soluble signaling proteins of varied growth factors.[7] Consequently, morphological mimicking of nanofiber scaffolds, when coupled with controlled growth-factor delivery function, can provide both morphological/micromechanical and biochemical clues for the assembly of regenerating tissue within a controllable nano-/microenvironment. However, in this context, research is still quite limited, although use of electrospun nanofibers for drug releases for pharmaceutical applications has been reported. For example, Kenawy et al.[8] studied the release of 5% tetracycline hydrochloride from electrospun poly(ethylene-*co*-vinyl acetate), poly(lactic acid), and their blends. Verreck et al.[9] incorporated poorly water-soluble drugs of itraconazole and ketanserin into polyurethane nanofibers for potential use in topical drug administration and wound healing. Zong et al.[10] prepared electrospun poly(D,L-lactic acid) fibers containing an antibiotic drug, Mefoxin, applicable for prevention of post-operation-induced adhesion. Jiang et al.[11] investigated the releases of ibuprofen-loaded composite membranes composed of poly(lactide-*co*-glycolide) (PLGA) and poly(ethylene glycol)-*g*-chitosan (PEG-*g*-CHN) for possible atrial tissue applications. Luu et al.[12] demonstrated plasmid DNA could be incorporated into poly(lactide-*co*-glycolide) random copolymer and poly(D,L-lactide)−poly(ethylene glycol) block copolymer for therapeutic application in gene delivery for tissue engineering. Only recently, Leong's group[13] demonstrated functionalizing nanofibers for tissue engineering applications by incorporation of human β-nerve growth factor (NGF) into a copolymer of ϵ-caprolactone and ethyl ethylene phosphate (PCLEEP) followed by an in vitro release study and bioactivity assessment.

* To whom correspondence should be addressed: tel +65-6516 6567; fax +65-6874 6567; e-mail biezyz@nus.edu.sg.

† Division of Bioengineering, National University of Singapore.

‡ Department of Mechanical Engineering, National University of Singapore.

§ Nanoscience and Nanotechnology Initiative, National University of Singapore.

|| Institute of Materials Research and Engineering.

10.1021/bm050743i CCC: $33.50
Published on Web 03/09/2006

All of the aforementioned release work adopted the route of simply mixing drugs and carrier polymers for electrospinning of drug-incorporated nanofibers. However, the major disadvantage of this blend-electrospinning procedure is that the blend formulation would usually result in severe burst release phenomenon, as has been reported.[8,10,12] Burst releases lead to higher initial drug delivery and reducing the effective lifetime of the device.[14] Many investigations using nanofibers for controlled release applications have demonstrated the weakness of the blend-electrospinning method and highlighted the significant role of drug−carrier interaction in controlled releases.[12,15−17] Another disadvantage is that, during preparation of the spinning solution and the blend-electrospinning process, the long time exposure of bioactive proteins to harsh organic solvent environment would potentially make proteins denatured to lose its biological activity. Therefore, it would be beneficial to address the raised issues by encapsulating or entrapping the drugs inside the nanofibers. In practice, presently there is also an increasing need to produce drug-encapsulated nanofibers for potential applications in biomedical areas. These include preserving an unstable biological agent from an aggressive environment, for example, in wound healing treatment to prevent the decomposition of a labile compound under a harsh environment, and to deliver a biomolecular drug in a sustained fashion. Recently, it has been demonstrated that the release profile of drugs can be ideally controlled to perform nearly zero-order kinetics by using compatible drugs with polymers[16,17] or controlled by making a post-electrospinning coating treatment[18] to form a coat over the drug-containing nanofiber surface. Despite these available approaches, newly emerged coaxial electrospinning[19−22] would provide an alternative and simple means to encapsulate drugs. With coaxial electrospinning, two components can be coaxially and simultaneously electrospun through different feeding capillary channels to generate composite nanofibers in the form of core−sheath structure. Ideally, drugs or biologically active agents in the core−sheath-type nanofibers can be released through the shell if the shell polymer is sufficiently permeable to the drug molecules wrapped. Or, they can be held over a period of time until release when the carrier polymer starts to degrade. However, use of core−sheath-structured nanofibers for encapsulating bioactive substances and conducting controlled releases has yet to be explored.[23]

This study first investigated the feasibility of encapsulating a nonelectrospinnable model protein (i.e., fitcBSA) along with a water-soluble poly(ethylene glycol) (PEG) into biodegradable poly(ϵ-caprolactone) (PCL) nanofibers via the coaxial electrospinning technique and a variety of characterization methods. Next, an in vitro release study was preliminarily conducted to demonstrate the efficacy of using core−sheath composite nanofibers for sustained releases. For comparative purposes, the same materials used in the coaxial electrospinning were blended, homogeneously dispersed and electrospun into blend type composite nanofibers using the conventional single fluid electrospinning method.

2. Experimental Section

2.1. Materials. Granular PCL (M_n 80K, Aldrich) polymer, fluorescein isothiocyanate-conjugated bovine serum albumin (fitcBSA, molecular weight 67K), and organic solvent 2,2,2-trifluoroethanol (TFE) (purity ≥99.0%, Fluka, Buchs, Switzerland) were purchased from Sigma−Aldrich, Inc. (St. Louis, MO). Poly(ethylene glycol) (PEG, M_n 35K) was obtained from Merck. Transparent PCL/TFE solution (12% w/v), as shell fluid for coaxial electrospinning, was made by dissolving certain amounts of PCL in TFE with sufficient stirring at room temperature. To prepare core solution of fitcBSA/PEG, 5 mg of fitcBSA was dissolved in 5 mL of deionized water, followed by addition of 500 mg of PEG.

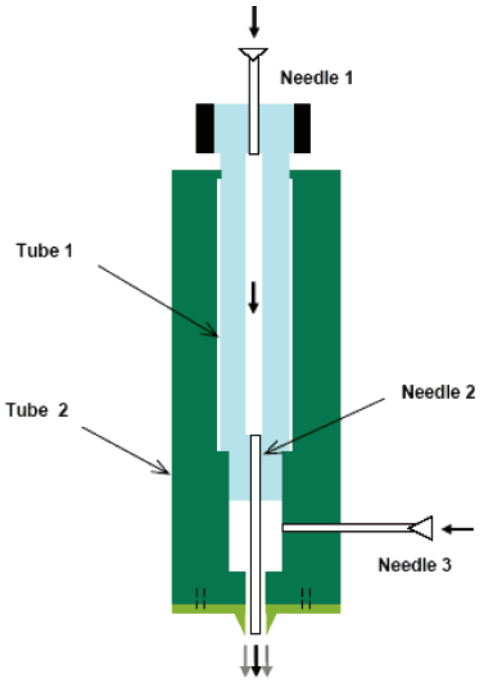

Figure 1. Schematic illustration of a homemade coaxial electrospinning spinneret used in preparing our PCL-r-fitcBSA/PEG core−sheath nanofibers (PCL-r-fitcBSA/PEG denotes the core fitcBSA/PEG is wrapped inside the PCL sheath).

2.2. Electrospinning. One of the key components in the coaxial electrospinning setup is a compound spinneret, consisting of two (or more) small-diameter capillary tubes with one located inside another. Figure 1 shows our homemade coaxial electrospinneret used in this study. The subassemblage of copper tube 1 and steel needles 1 and 2, which is also used as the electrode for charging the spinning dopes by applying high voltage at needle 1, forms the feeding channel for the inner fluid. The outer fluid goes through the side needle 3 mounted through the Teflon wall of tube 2. The exit orifice diameters of the inner and outer capillaries are 1.1 and 2.5 mm, respectively. The general features of this customized electrospinneret are (1) better concentricity for the concerned inner and outer capillaries; (2) controllable flow rates for both the inner and outer dopes, respectively; (3) adjustable protruding length of the inner capillary along the axis; and (4) changeable tubular gap between the openings. This design would facilitate operational adjustment in getting a stable compound spinning jet and offers a possibility to conduct detailed investigation on the coaxial electrospinning process. In coaxial electrospinning, the output electrode from a high-voltage supply (RR50-1.25R/230/DDPM, Gamma High Voltage Research) was clipped at needle 1 to charge the polymer solutions, while two precision syringe pumps (model 100, KD Scientific Inc.) were employed to separately control the inner and outer flow rates. Our customized setup allowed the fitcBSA/PEG to be encapsulated in PCL nanofibers to generate PCL-r-fitcBSA/PEG composite nanofibers with processing parameters listed in Table 1. For comparison purpose, composite nanofibers of PCL/fitcBSA/PEG blend were also prepared from a normal electrospinning method as described previously.[24] To have the same constitutional ratio of the components in the PCL/fitcBSA/PEG nanofibers as the coaxially electrospun PCL-r-fitcBSA/PEG nanofibers, solutions of the PCL/TFE and aqueous fitcBSA/PEG used in coaxial electrospinning were mixed at ratios of 1.8:0.2, 1.8:0.4, and 1.8:0.6 for preparing samples M0.2, M0.4, and M0.6, respectively. The processing parameters were also listed in Table 1.

Table 1. Processing Variables for Nanofibers of Core−Shell Structured PCL-r-fitcBSA/PEG and Blended PCL/FitcBSA/PEG*

Sample code	Gap distance, cm	Flow rate, mL/h Inner	Flow rate, mL/h Outer	Applied voltage, kV	Ambient temperature, °C	Ambient humidity, %
0.2	13	0.2	1.8	10.1	22.7	78
0.4	13	0.4	1.8	10.3		
0.6	13	0.6	1.8	10.6		
M0.2	10.5	1.09		6.4	22.1	79
M0.4	10.5	1.16		6.8		
M0.6	10.5	1.25		7.3		

* Samples of 0.2, 0.4, and 0.6 were prepared from coaxial electrospinning using the setup in **Figure 1**; while M0.2, M0.4, and M0.6, prepared from a normal electrospinning process, possess same component ratios as that of core−shell structured ones, respectively. The loadings of fitcBSA in the electrospun composite nanofibers were calculated to be 0.85 mg/g (samples 0.2 and M0.2), 1.56 mg/g (samples 0.4 and M0.4), and 2.17 mg/g (samples 0.6 and M0.6).

2.3. Characterization. 2.3.1. Scanning Electron Microscopy. The electrospun nanofibrous membranes, mounted on metal stubs by using conductive double-sided tape, were sputter-coated with gold up to 90 s in a JEOL JFC-1200 fine coater. Their morphologies were then observed by use of a scanning electron microscope (JEOL JSM-5600, Japan) at an accelerating voltage of 15 kV. Fiber diameters of the nanofibrous membranes were analyzed with image visualization software, ImageJ, developed by the Upper Austria University of Applied Sciences. Totals of 90−100 counts were used to calculate the distribution percentages.

2.3.2. Laser Confocal Scanning Microscopy. To confirm the presences and distribution of fluorescent-labeled BSA in the PCL nanofibers, observations of PCL-r-fitcBSA/PEG nanofibers deposited on microscope glass slides were performed on a laser confocal scanning microscope (LCSM, Leica TCS SP2, Germany). The excitation and emission wavelengths were 488 and 535 nm, respectively. When the composite nanofibers were observed under LSCM, pure PCL fibers were used as negative control: in brief, first to adjust all the parameters including the laser intensity and gain, until fluorescent signals cannot be seen from the pure PCL fiber sample; then without changing any settings, the same parameters were used to observe the fitcBSA-containing nanofiber samples.

2.3.3. Transmission Electron Microscopy. The core−sheath structure of the coaxially electrospun PCL-r-fitcBSA/PEG composite nanofibers was examined on a JEOL JEM-2010F FasTEM field emission transmission electron microscope, operated at 100 kV. The samples for TEM were prepared by directly depositing the as-spun nanofibers onto copper grids, which were coated in advance with supportive Formvar films and carbon. The samples were kept in a vacuum oven for 48 h for drying at room temperature before TEM imaging.

2.3.4. X-ray Photoelectron Spectroscopy. X-ray photoelectron spectroscopy (XPS), also known as electron spectroscopy for chemical analysis (ESCA), is a widely used chemical analysis technique. It is able to determine the chemical composition of sample surface for all elements except hydrogen with a typical sampling thickness <5−10 nm. XPS analysis of the coaxially electrospun PCL-r-fitcBSA/PEG nanofibers was conducted on a VG Escalab 2201-XL Base System (Thermo VG Scientific, England) with a takeoff angle of 90°.

2.4. In Vitro Release. The nanofibrous PCL-r-fitcBSA/PEG and PCL/fitcBSA/PEG membranes were first punched into small circles (diameter 8 mm) with a Ribbel biopsy punch. The circles with a total mass of ca. 36.5 mg were immersed in 5 mL of PBS (pH = 7.4) at 37 °C. At predetermined time intervals, the release buffer was completely removed for analysis and 5 mL of fresh PBS was replenished for continuing incubation. The fitcBSA amount present in the release buffer was determined by a Tecan Specta Fluor Plus microplate reader (λ_{ex} 485 nm, λ_{em} 535 nm). The results were presented in terms of cumulative release as a function of release time:

$$\text{cumulative amount of release, \%} = \frac{M_t}{M_\infty} \times 100 \qquad (1)$$

where M_t is the amount of BSA released at time t and M_∞ is the total amount of BSA in the nanofibrous membranes. All samples were run in triplicate.

At the end of the release study, water from the remaining samples was gently removed by tissue paper and each sample was dissolved in 3 mL of methylene chloride. The residual protein was then extracted from the organic phase to the aqueous phase by adding 3 mL of PBS. The amount of protein extracted was similarly assayed as described above. The morphology of the post-release samples were assessed on a high-resolution Quanta FEG 200 field emission scanning electron microscope (FESEM) (FEI Co,), operated at an acceleration voltage of 8−10 kV.

3. Results and Discussion

3.1. Fiber Morphology. In terms of forming a fibrous structure, the pure BSA was found to be nonelectrospinnable. This however, would not be a prerequisite for generating nanofibers in the coaxial electrospinning process, as the major role in fiber forming would be the shell solution used. Shown in Figure 2 is the nanofibrous morphology of coaxially electrospun PCL-r-fitcBSA/PEG, prepared under stable processing conditions, that is, no dripping of droplet, formation of a stable Taylor cone at the exit orifice of the compound spinneret, and continuous jet ejection during the coaxial electrospinning. The SEM images illustrate that these nanofibers, despite produced at varied inner flow rates, possess a common feature of being bead-free, randomly arrayed, and very porous. Although the inner solution of fitcBSA/PEG was also found to be nonelectrospinnable in this study, it has little influence on the formation of fibrous structure from the compounded inner and outer fluids. Moreover, measurement of the fiber diameters of the coaxially electrospun PCL-r-fitcBSA/PEG indicates that alteration of inner flow rates from 0.2 to 0.6 mL/h resulted in fiber size increase as shown in Figure 3. The correlation between flow rate and fiber size increase can be attributed to the extrudate swell effect of viscoelastic polymers in the extrusion process. This is usually affected by factors such as concentration, extrusion rate, nozzle length, addition of stiffer fillers, temperature, etc. The swell effect would be simultaneously passed to the shell fluid by expansion of the shell to a certain extent. This could consequently affect the stretching ability of the jet in the instability development zone. Previous investigations have indicated that the bending instability in the electrospinning is responsible for the formation of nano- or submicroscaled ultrafine fibers.[25,26] The swell effect would be absent if the inner fluid is not of the viscoelastic type. For example, in another of our recent studies, FePt nanoparticles dispersed in hexane were encapsulated in the PCL nanofibers. A variation of inner flow rate actually did not affect the overall fiber diameters.[27,28]

The blend-type composite nanofibers of PCL/fitcBSA/PEG (i.e., samples M0.2, M0.4, and M0.6) were prepared by a normal electrospinning method and possessed the same component ratio as that of PCL-r-fitcBSA/PEG. However, it was found they exhibited beaded fiber morphologies (Figure 4) although they were prepared under stable processing conditions. The measured fiber diameters of PCL/fitcBSA/PEG blend are slightly smaller than that of core−shell-structured PCL-r-fitcBSA/PEG; however, the presence of larger beads would counteract the merits of its smaller size contribution to properties of surface area and

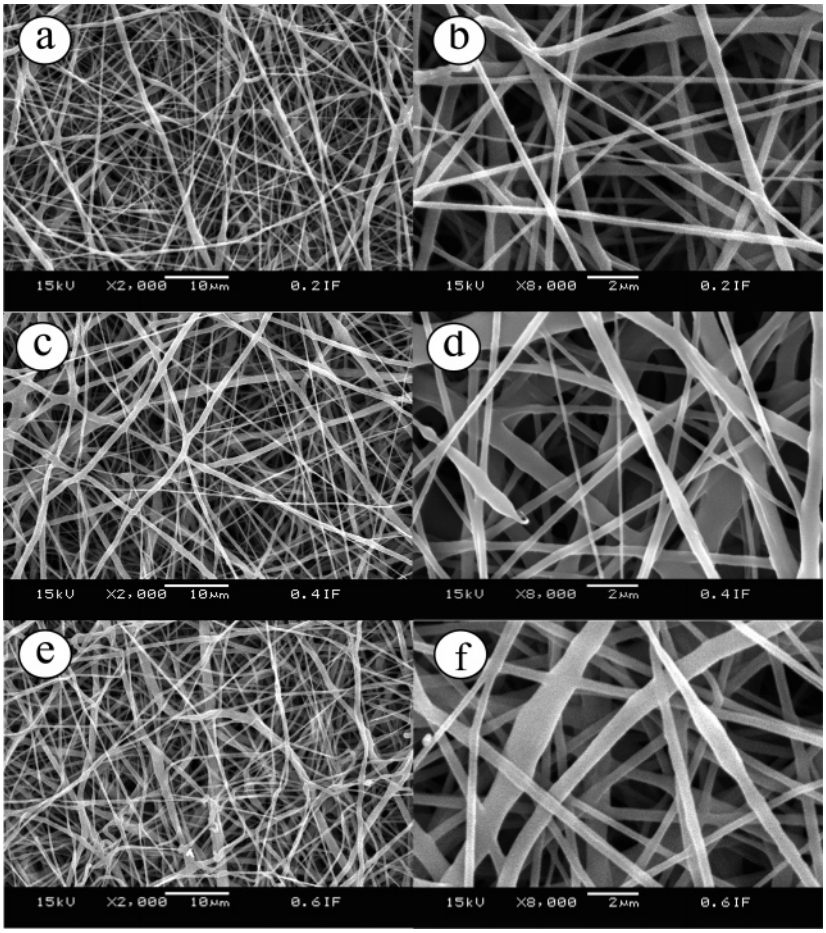

Figure 2. Coaxially electrospun PCL-r-fitcBSA/PEG nanofibers prepared with inner flow rates of 0.2 (a, b), 0.4 (c, d), and 0.6 mL/h (e, f). The outer flow rate used was maintained at 1.8 mL/h in all cases. The magnifications in the images are 2000× (a, c, e) and 8000× (b, d, f).

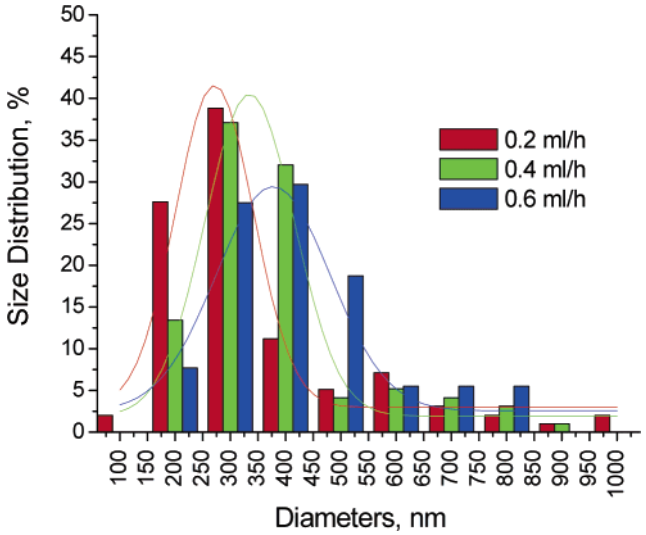

Figure 3. Size distributions of PCL-r-fitcBSA/PEG composite nanofibers prepared at different flow rates. The fiber diameters for samples 0.2, 0.4, and 0.6 are 277 ± 140, 330 ± 167, and 378 ± 149 nm, respectively.

mechanical performance. Random blending had compromised the resultant nanofiber morphology, suggesting that the non-electrospinnability of fitcBSA/PEG has a pronounced influence on the normal electrospinning process. This result, in contrast, further demonstrated that coaxial electrospinning is of particular advantage for those materials that will not form fibers via the normal electrospinning process.[19,29]

3.2. Characterization of the Encapsulation. As the SEM images in Figure 2 cannot provide evidences that fitcBSA/PEG was successfully encapsulated inside the nanofibers, several means to characterize this encapsulation effect were employed. First, LCSM showed that all the PCL-r-fitcBSA/PEG composite nanofibers emitted fluorescence (Figure 5), suggesting the presence of fluorescent-labeled BSA protein in the coaxially electrospun nanofibers. The fibrous morphology without bead defects is also consistent with SEM observation shown in Figure 2. Under LCSM, fibers and beads of the PCL/fitcBSA/PEG blend nanofibers also exhibited green color, with beads being brighter. Previously, the presence of fluorescence was used to identify core−shell structure in microspheres with a large diameter of a few hundreds micrometers.[30] However, since the PCL-r-fitcBSA/PEG nanofiber is extremely small, detailed layer structure on the inner component distribution cannot be clearly identified by LCSM. Therefore, TEM observation was further conducted to obtain direct evidence that fitcBSA/PEG was indeed encapsulated within the shell material of PCL (Figure 6). It can be seen that while the inner component was properly wrapped in the center of composite nanofibers of PCL-r-fitcBSA/PEG (Figure 6a), there are also cases of irregular movement of inner component, as shown in Figure 6b, with an obvious slanted portion very close to the fiber surface as shown in the observed TEM segment. We also found that the inner fluid seemed to affect the overall fiber morphology as shown in Figure 6c. The size of the inner component fluctuated along the fiber axis with the shell shape being adjusted correspondingly. This would potentially disturb the stretching ability of the compounded jet during the electrospinning process as

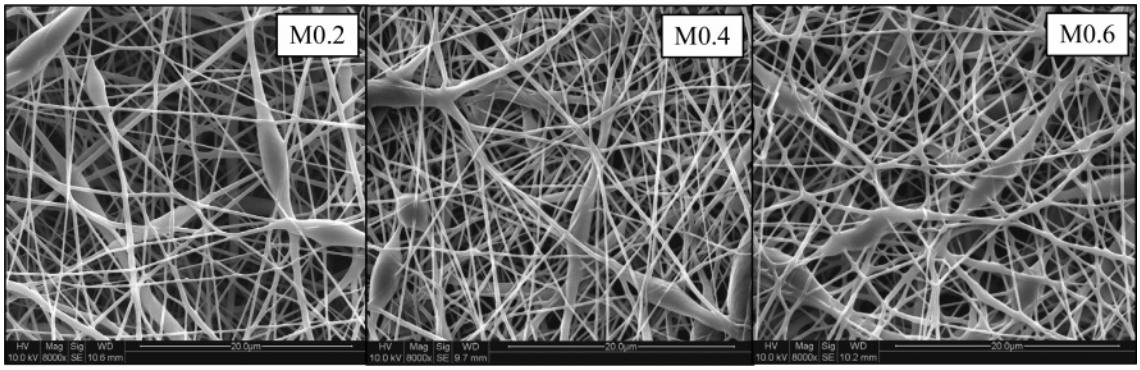

Figure 4. Fiber morphologies of electrospun PCL/fitcBSA/PEG blend nanofibers. The M0.2, M0.4, and M0.6 samples possessed the same composition ratios as those of samples 0.2, 0.4, and 0.6, respectively. The fiber sizes for M0.2, M0.4 and M0.6 are 255 ± 86, 277 ± 87, and 291 ± 87 nm, respectively.

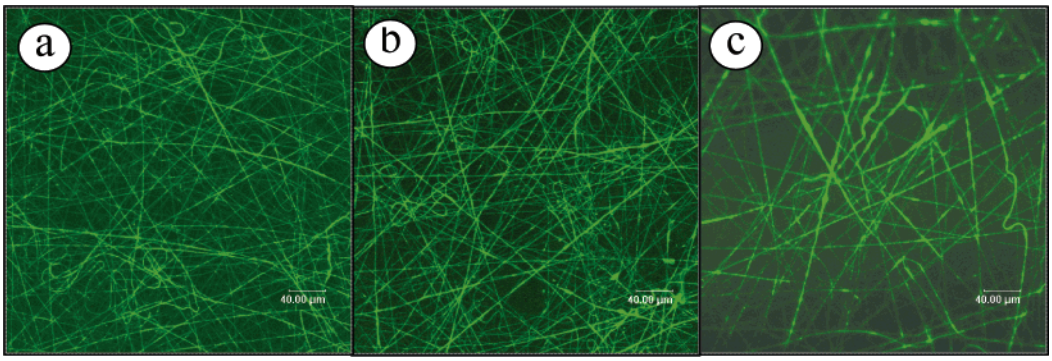

Figure 5. Laser confocal microphotographs of core−sheath PCL-r-fitcBSA/PEG composite fibers electrospun at inner flow rates of 0.2 (a), 0.4 (b), and 0.6 mL/h (c). The outer flow rate used was 1.8 mL/h.

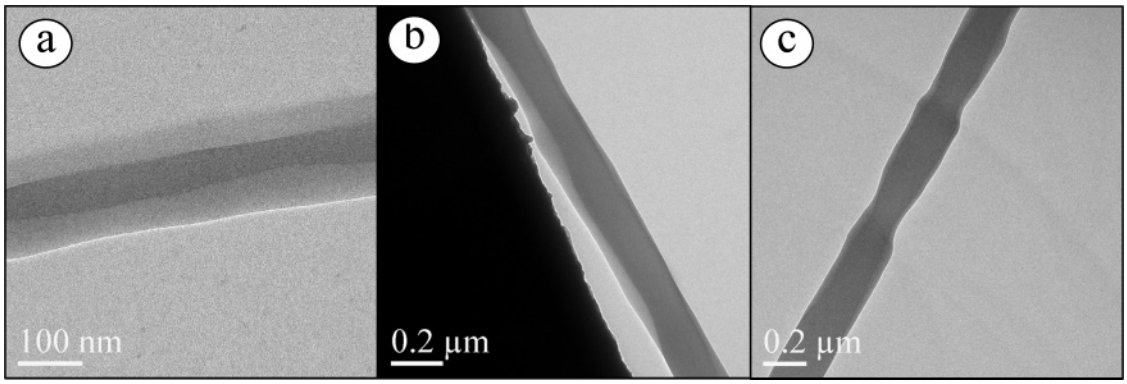

Figure 6. Typical TEM images of coaxially electrospun PCL-r-fitcBSA/PEG nanofibers produced from varying inner flow rates of 0.2−0.6 mL/h and with outer flow rate of 1.8 mL/h: (a) core component properly located in the center, (b) irregular movement of core component, and (c) fluctuated fiber shape.

discussed in section 3.1. Sharp boundaries in the TEM images essentially reflect the difference of electron transmission ability between the core and shell materials. The likely reasons to form sharp boundaries are associated with the immiscibility of the two polymer fluids and the very fast processing characteristic of electrospinning, which would prevent the two fluids from mixing significantly.[19,20,29]

Apart from those clearly observed core−shell fibers, TEM images of this coaxially electrospun PCL-r-fitcBSA/PEG also showed some fibers that did not exhibit any core in the fiber (or the core cannot be seen). We suggest two possible reasons for this phenomenon: (1) during the coaxial processing, as happened in a normal electrospinning,[31] there appeared subjets (branching) that were offshoots from the shell fluid of the main compounded fluidic jet. This is true especially for the smaller noncore nanofibers (e.g., diameters <100 nm). (2) It would have a connection with the underlying mechanism of wrapping a core component inside the sheath during the coaxial electrospinning process. The groups of both Xia[22] and Yarin[19] groups have proposed an entrainment mechanism. From a recent calculation,[32] we speculate that all free charges in the two fluids upon charging would leave the liquid−liquid interface very rapidly and migrate to the outer free surface upon having high potential applied. The Maxwell stress would therefore stretch the outer fluid as that occurring in a normal electrospinning. The inner fluid would be entrained only by the viscous dragging-like stresses and/or contact friction in the inter-phase imposed from the rapid stretching of the shell fluid during coaxial electrospinning.[19,22] Since the coaxial electrospinning is a dynamic process, factors such as flow rate of the inner and outer fluids, interfacial tension, and viscoelasticity of the two polymer fluids could affect the entrainment and produce noncore fibers. It is suggested that an optimal processing condition may exist where continuous core−shell-structured bicomponent composite nano-

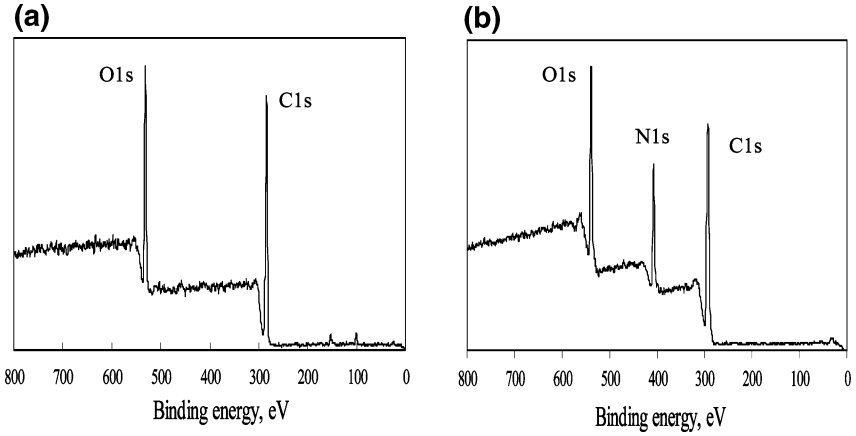

Figure 7. (a) Typical XPS spectrum of PCL-r-fitcBSA/PEG core−sheath composite nanofibers. Atomic ratio in the samples of 0.2, 0.4, and 0.6 is 26.49% ± 1.43% for O1s and 73.50% ± 1.43% for C1s. (b) XPS spectrum of protein containing blend nanofibers.

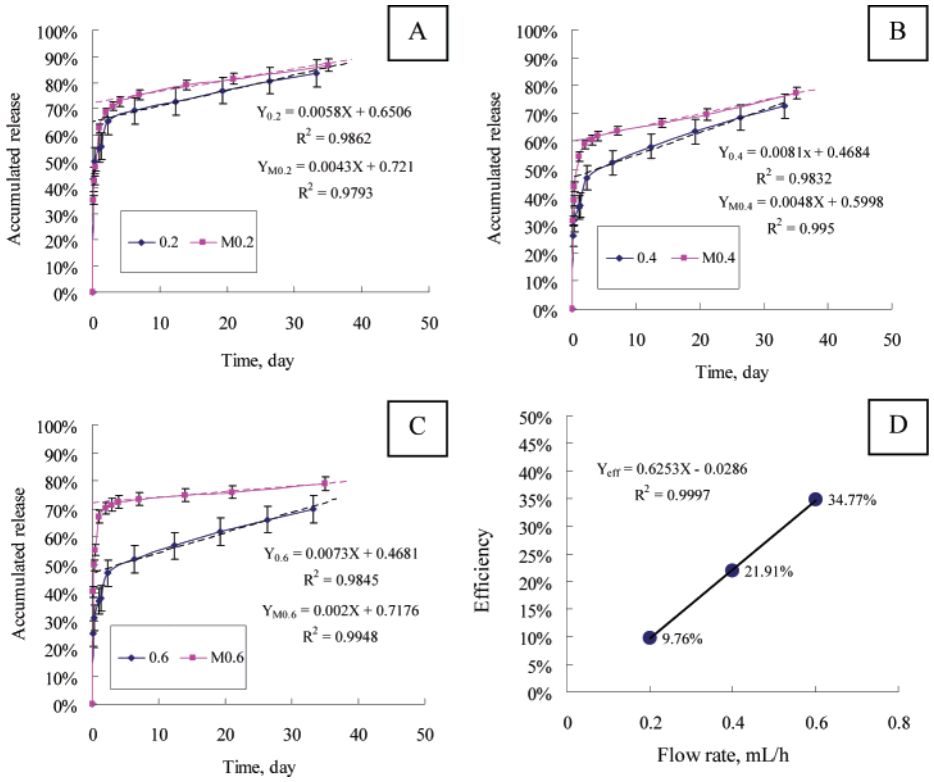

Figure 8. Compared with PCL/fitcBSA/PEG blend nanofibers, PCL-r-fitcBSA/PEG showed burst release suppression effect. (A) Comparison between samples 0.2 and M0.2; (B) comparison between samples 0.4 and M0.4; (C) comparison between samples 0.6 and M0.6; (D) suppression efficiency vs flow rate/loading. The BSA loadings for samples 0.2 and M0.2, 0.4 and M0.4, and 0.6 and M0.6 are 0.85, 1.56, and 2.17 mg/g, respectively.

fibers from the main jet can be produced. Existence of noncore fibers was also observed in the work of Yu et al.[29] Obviously, coaxial electrospinning is far more complex than normal single-fluid electrospinning. The complex electrohydrodynamics involved have yet to be illustrated by more experimental and theoretical investigations.

To further confirm the encapsulation of fitcBSA/PEG inside PCL nanofibers rather than being exposed on the nanofiber surface, XPS analysis technique was used to examine the chemical characteristics on the surfaces of PCL-r-fitcBSA/PEG composite nanofibers. Figure 7a shows a typical XPS spectrum of the coaxially electrospun PCL-r-fitcBSA/PEG composite nanofibers. As expected, there are only C 1s and O 1s peaks presented at binding energies of ca. 285 and 530 eV, respectively. Moreover, the peak area ratio of O 1s/C 1s was also found to be in good agreement with the theoretical values of O/C in PCL. These results suggested that fitcBSA/PEG was properly wrapped by the shell material PCL, and the shell thickness is at least beyond the ultimate detection depth of XPS, i.e., 5−10 nm. Comparatively, nanofibers from blending of protein and PCL would generate an extra characteristic N 1s peak at 400 eV (Figure 7b).

3.3. In Vitro Release. Release performance differences between PCL-r-fitcBSA/PEG and PCL/fitcBSA/PEG were plotted in Figure 8 and compared on the basis of the same protein loadings. The release kinetics for all cases can be illustrated by two stages: an initial fast release before the inflections (stage I) followed by a constant linear release (stage II). In stage I, there were initial burst releases from both composite nanofibers with averaged release amounts of 35.7% in 3 h for PCL/fitcBSA/PEG and 31.2% in 4 h for PCL-r-fitcBSA/PEG. Burst release in PCL/fitcBSA/PEG is obviously more severe than that of

encapsulation formulation. After this initial burst release, protein was approximately linearly released (stage II) with PCL-r-fitcBSA/PEG being released faster than that of PCL/fitcBSA/PEG. If it is assumed that the intercepts of the linear curves were associated with the burst release phenomena, it was found that the initial fast release in a period of 2 days for the composite nanofibers of PCL/fitcBSA/PEG blend accounts for 60−70%, versus 45−65% for the core−sheath-structured PCL-r-fitcBSA/PEG. Incorporation of BSA by blending-electrospinning is worse than that for the encapsulation mode. Encapsulation therefore would suppress the burst release. The suppression efficiency can simply be expressed by

$$\text{suppression efficiency (\%)} = \frac{\text{intercept of } Y_{Mi} - \text{intercept of } Y_i}{\text{intercept of } Y_{Mi}} \times 100 \quad (2)$$

where $i = 0.2$, 0.4, or 0.6. On the basis of eq 2, the suppression efficiency versus flow rate (loadings) was plotted in Figure 8D. The perfect linearity indicates the suppression efficacy is proportional to the loadings. This is understandable as smaller loading in terms of current blending formulation is almost equivalent to an encapsulation effect, while higher loading will be able to form channels for agent to release faster from the device. After the initial fast release, both formulations were able to release proteins at constant releasing rates. However, sustainability between both formulations is different. PCL/fitcBSA/PEG could not sustain a sufficient amount of release over a long time, resulting in reduced effective lifetime of the releasing device. For example, before their common intersection points of the linear ranges are reached, encapsulated release devices, that is, the core−shell-structured nanofibers, can sustain a higher amount of releases of 27−35%. In contrast, the incorporated ones support only about 10−20%. Our current study indicates that use of core−sheath structured devices can apparently alleviate the initial burst release and improve the sustainability of nanofiber-based releasing devices. This conclusion is also in agreement with results obtained from other similar core−shell-type configurations such as microspheres and fibers.[18,30,33,34]

At the end of the in vitro release study (approaching 100%), both the PCL-r-fitcBSA/PEG and PCL/fitcBSA/PEG nanofibers were observed by high-resolution SEM. Interestingly, the fiber morphology of PCL/fitcBSA/PEG (Figure 9d−f) has changed from previously smooth surfaces (images not shown) to very rough and eroded-like with very obvious pits and/or cavities presented. The severity is obviously related to the incorporated amount of fitcBSA/PEG. Since the fitcBSA/PEG aggregates are water-soluble, it is believed that the pits/cavities were formed from the dissolution of the fitcBSA/PEG aggregates presented on and in the fiber. However, this did not happen for the coaxial electrospun PCL-r-fitcBSA/PEG nanofibers. The only change, compared to its pristine form, is that the PCL-r-fitcBSA/PEG fibers became flatter and collapsed from their previous cylindrical shape (Figure 9a−c). This may arise from the exhausted state of fitcBSA/PEG aggregates inside the PCL shell. The different post-release morphologies in both composite nanofibers would therefore relate to their respective distribution manners of the fitcBSA/PEG aggregates in the composite nanofibers due to different techniques used for nanofiber preparations, and consequently different delivery fashions or mechanisms during the in vitro releasing process.

The underlying mechanism of releases in both cases in our current release time scale is less likely to be governed by the polymer degradation. This is because the PCL polymer would withstand a very long time (>2 years) for it to be hydrolytically degraded. The possible mechanism will therefore be Fickian diffusion through the polymer matrix and/or diffusion through pores in the matrix.[35] On the basis of the preceding release kinetics and post-release morphological observations (Figures 8 and 9), it would be relatively easy to understand the release mechanism of current PCL/fitcBSA/PEG blend formulation because it is similar to a monolithic release device,[36] which is usually fabricated by randomly dispersing the protein within a solid continuous matrix of polymer. The possible mechanism is that as the fitcBSA/PEG aggregates presented on or adjacent to the nanofiber surfaces were dissolved and diffused out of the matrix, cavities are consequently formed that will permit the solvent front to penetrate to the aggregates located deeper within the matrix. The initial fast release of protein in stage I (Figure 8) would be related to dissolution of BSA/PEG within the surface vicinity, and the linear release in stage II (Figure 8) could be of diffusion from the deeper regions of the polymer matrix. This process is loading-dependent. For example, at high loadings (e.g., for cases of M0.4 and M0.6), release become aggressively erosionlike. Loading levels that affect the microstructure alterations in the monolithic dispersion systems have been theoretically described by percolation theory.[37−39] Loadings of soluble fitcBSA/PEG aggregates in this study are in the range of 9−22%. For even higher loadings, for example, up to 50%, the leaching release would actually provide a convenient means to prepare 3-D porous nanofibers with nanotopographical surface features and pronounced increase in surface area as demonstrated elsewhere.[40]

Unlike PCL/fitcBSA/PEG, core−shell-structured PCL-r-fitcBSA/PEG nanofibers belong to the reservoir-type release device, in which the drugs are encapsulated by a polymer shell (similar to a coating) that would be able to regulate the rate of release. Reservoir devices have the advantages of providing a constant rate of release over a substantial portion of their lifetime and higher loading level of active agents than most other systems.[36] However, reservoir release rate is also critically dependent on shell/coating thickness, surface area, permeability, and defects such as thin spots and pinholes. The reason behind the release mechanism of current core−sheath nanofibers is not clear. We hypothesize that the core materials of fitcBSA/PEG would preferably diffuse out through the nonsealed cutting openings[41] of the small circles (diameter 8 mm) and the imperfections of core−sheath structure such as very thin shell to favor good permeability (Figure 6b), the pinholes, and the shell failure (Figure 9a−c). The burst release in the initial stage is also possibly associated with the coencapsulation of PEG, which can be used to modulate the release rate.[42] PEG in the present study was to stabilize the protein and increase the viscosity so as to stabilize the compound jets during coaxial electrospinning. Since PEG is a hydrophilic and water-soluble polymer, the protein in the fitcBSA/PEG aggregates will be released simultaneously as the physically entangled PEG slowly dissolve in the buffer. However, inclusion of the relatively large amount of water-soluble PEG in the core−sheath device would potentially give rise to an osmotic effect to pump the inner agents out as the membranes were hydrated/wetted and water molecules penetrate into the core, causing dilution and swelling of the inner components to diffuse out rapidly.[36] Both the PCL-r-fitcBSA/PEG and PCL/fitcBSA/PEG nanofibers exhibited fast release phenomena in the initial 2 days. This is partially contributed by the very high surface-area-to-volume ratio of the nanofibrous membrane, as high surface area would aid in mass

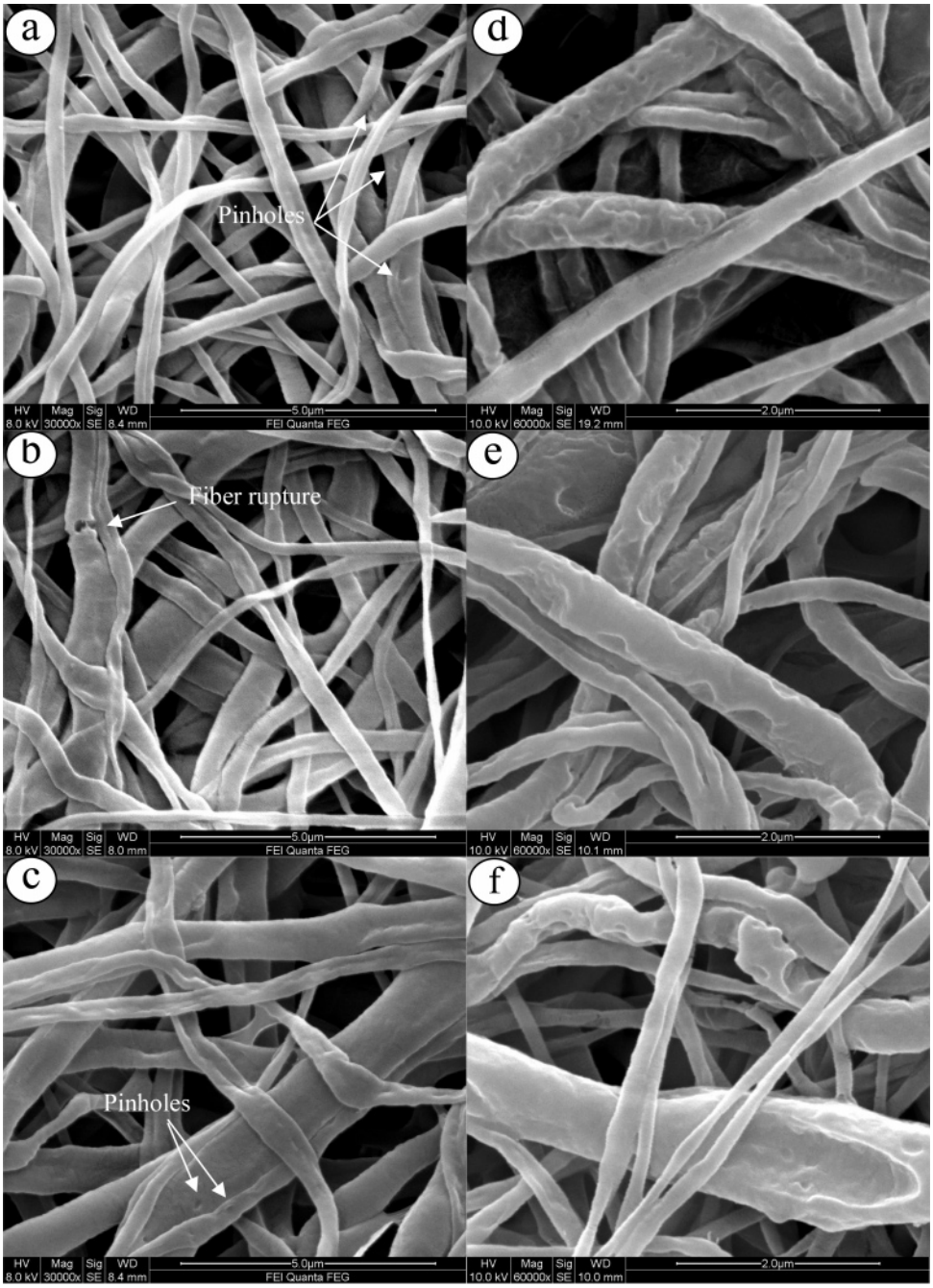

Figure 9. High-resolution SEM images of fitcBSA contained PCL nanofibers after releasing 176 days for samples of (a) 0.2, (b) 0.4, and (c) 0.6 and 149 days for samples of (d) M0.2, (e) M0.4, and (f) M0.6. The mass percentages of fitcBSA/PEG in these composite nanofibers are 8.6%, 15.8%, and 21.9% with respect to samples of (0.2, M0.2), (0.4, M0.4), and (0.6, M0.6), respectively.

transfer and efficient drug release.[8,9,11] Release device size plays an important role in controlling the initial release of the protein.[43]

Many important factors (e.g., the protein properties, co-encapsulated molecules, polymer matrix, and the interactions among them, etc.) have influences on the drug/protein release kinetics. Encapsulation by formation of core−sheath-compounded nanofibers will provide an alternative strategy for moderating the release rate of drug release. Notably, it would be more effective than other forms of devices due to its nanoscale size, which implies less possibility of introducing fabrication-related defects and higher surface area for mass transfer, and protective function for preserving the activity of the agents encapsulated. Although this work has not examined the protein integrity of the released BSA, it is expected that its structure released from PCL-r-fitcBSA/PEG formulation would remain the same or at least superior to the one from blend-electrospinning. This is because many studies based on nanofibers prepared from electrospinning of drug and carrier blends have shown evidence that the chemical structure after electrospinning appears to be identical.[15,44] The bioactive agents such as DNA after release was intact,[12] the α-chymotrypsin enzyme immobilized on the polystyrene nanofibers retained high activities in both aqueous and organic media,[45] and the drug functionality seems to be completely unaffected by the gentle electrospinning process.[10] On the other hand, the core−sheath structure and coaxial electrospinning itself apparently and substantially reduces the possibility of contact with bioactive agents or exposure to the organic solvents, which would protect proteins from activity loss. This protective role would also work similarly during the release process. In this regard, Zeng et al.[18]

has recently demonstrated that the enzyme activity of luciferase released from poly(*p*-xylene)-coated composite nanofibers remained intact.

4. Conclusions

Fluorescent-labeled BSA protein along with PEG has been successfully encapsulated in the PCL nanofibers in the form of core−sheath structure by a coaxial electrospinning technique. Such a layer structure was characterized by TEM, LCSM, and XPS. For the coaxial electrospinning process, it was found that varying inner flow rate of fitcBSA/PEG/TFE solution from 0.2 to 0.4 to 0.6 mL/h led to an increase in the overall diameter of PCL-r-fitcBSA/PEG nanofibers from ca. 270 to 330 to 380 nm, respectively. In vitro release study indicated that the core−shell-structured nanofibers are capable of releasing the BSA protein continuously over a period of more than 5 months. The release rate was fiber size-dependent: smaller-sized fibers have a faster release rate than larger ones. Compared to the nanofibers of fitcBSA/PEG/PCL blend, core−shell-structured PCL-r-fitcBSA/PEG nanofibers could obviously suppress the burst release. The suppression efficiency was loading-dependent. SEM examination of post-release samples suggested the release kinetics are diffusion-controlled but are obviously related to the dispersion fashions of the protein in the nanofibers. Present results provide a basis for further design and optimization of processing conditions to control the nanostructure of core−sheath composite nanofibers in order to achieve highly sustainable, controllable, and effective protein-releasing kinetics in practical tissue engineering applications. In this regard, coaxial electrospinning should be a viable technique for coupling the structural integrity and functionalization in one nanofiber to ultimately fulfill the success of using nanofibrous scaffolds for tissue regenerations.

Acknowledgment. We thank Mr. S. R. Godbole for his assistance in the coaxial spinneret design and Drs. Z. W. Ma and M. Kotaki for their help in XPS analysis. This study was supported by a research grant from the National University of Singapore.

References and Notes

(1) Reneker, D.; Chun, I. *Nanotechnology* **1996**, *7*, 216−223.
(2) Huang, Z.-M.; Zhang, Y.-Z.; Kotaki, M.; Ramakrishna, S. *Compos. Sci. Technol.* **2003**, *63*, 2223−2253.
(3) Li, D.; Xia, Y. *Adv. Mater.* **2004**, *16*, 1151−1170.
(4) Kadler, K. E.; Holmes, D. F.; Trotter, J.; Chapman, J. A. *Biochem. J.* **1996**, *316*, 1−11.
(5) Nishida, T.; Yasumoto, K.; Otori, T.; Desaki, J. *Invest. Ophthalmol. Vis. Sci.* **1988**, *29*, 1887−1890.
(6) Canty, E. G.; Kadler, K. E. *J. Cell Sci.* **2005**, *118*, 1341−1353.
(7) Baldwin, S. P.; Saltzman, W. M. *Adv. Drug Delivery Rev.* **1998**, *33*, 71−86.
(8) Kenawy, E.-R.; Bowlin, G. L.; Mansfield, K.; Layman, J.; Simpson, D. G.; Sanders, E. H.; Wnek, G. E. *J. Controlled Release* **2002**, *81*, 57−64.
(9) Verreck, G.; Chun, I.; Rosenblatt, J.; Peeters, J.; Dijck, A. V.; Mensch, J.; Noppe, M.; Brewster, M. E. *J. Controlled Release* **2003**, *92*, 349−360.
(10) Zong, X.; Kwangsok, K.; Dufei, F.; Shaofeng, R.; Hsiao, B. S.; Chu, B. *Polymer* **2002**, *43*, 4403−4412.
(11) Jiang, H.; Fang, D.; Hsiao, B.; Chu, B.; Chen, W. *J. Biomater. Sci., Polym. Ed.* **2004**, *15*, 279−296.
(12) Luu, Y. K.; Kim, K.; Hsiao, B. S.; Chu, B.; Hadjiargyrou, M. *J. Controlled Release* **2003**, *89*, 341−353.
(13) Chew, S. Y.; Wen, J.; Yim, E. K. F.; Leong, K. W. *Biomacromolecules* **2005**, *6*, 2017−2024.
(14) Huang, X.; Brazel, C. S. *J. Controlled Release* **2001**, *73*, 121−136.
(15) Kim, K.; Luu, Y. K.; Chang, C.; Fang, D.; Hsiao, B. S.; Chu, B.; Hadjiargyrou, M. *J. Controlled Release* **2004**, *98*, 47−56.
(16) Zeng, J.; Xu, X.; Chen, X.; Liang, Q.; Bian, X.; Yang, L.; Jing, X. *J. Controlled Release* **2003**, *92*, 227−231.
(17) Zeng, J.; Yang, L.; Liang, Q.; Zhang, X.; Guan, H.; Xu, X.; Chen, X.; Jing, X. *J. Controlled Release* **2005**, *105*, 43−51.
(18) Zeng, J.; Aigner, A.; Czubayko, F.; Kissel, T.; Wendorff, J. H.; Greiner, A. *Biomacromolecules* **2005**, *6*, 1484−1488.
(19) Sun, Z.; Zussman, E.; Yarin, A.; Wendorff, J.; Greiner, A. *Adv. Mater.* **2003**, *15*, 1929−1932.
(20) Zhang, Y.; Huang, Z.-M.; Xu, X.; Lim, C. T.; Ramakrishna, S. *Chem. Mater.* **2004**, *16*, 3406−3409.
(21) Loscertales, I. G.; Barrero, A.; Marquez, M.; Spretz, R.; Velarde-Ortiz, R.; Larsen, G. *J. Am. Chem. Soc.* **2004**, *126*, 5376−5377.
(22) Li, D.; Xia, Y. *Nano Lett.* **2004**, *4*, 933−938.
(23) Zhang, Y.; Lim, C.; Ramakrishna, S.; Huang, Z.-M. *J. Mater. Sci.: Mater. Med.* **2005**, *16*, 933−946.
(24) Zhang, Y. Z.; Ouyang, H. W.; Lim, C. T.; Ramakrishna, S.; Huang, Z.-M. *J. Biomed. Mater. Res., Part B: Appl. Biomater.* **2005**, *72B*, 156−165.
(25) Reneker, D. H.; Yarin, A. L.; Hao, F.; Koombhongse, S. *J. Appl. Phys.* **2000**, *87*, 4531−4547.
(26) Shin, Y. M.; Hohman, M. M.; Brenner, M. P.; Rutledge, G. C. *Polymer* **2001**, *42*, 9955−9967.
(27) Song, T.; Zhang, Y.; Zhou, T.; Lim, C. T.; Ramakrishna, S.; Liu, B. *Chem. Phys. Lett.* **2005**, *415*, 317−322.
(28) Song, T.; Zhang, Y. Z.; Zhou, T. J. *J. Magn. Magn. Mater.* **2005**, submitted for publication.
(29) Yu, J. H.; Fridrikh, S. V.; Rutledge, G. C. *Adv. Mater.* **2004**, *16*, 1562−1566.
(30) Rahman, N. A.; Mathiowitz, E. *J. Controlled Release* **2004**, *94*, 163−175.
(31) Koombhongse, S.; Liu, W.; Reneker, D. H. *J. Polym. Sci., Part B: Polym. Phys.* **2001**, *39*, 2598−2606.
(32) Reznik, S. N.; Yarin, A. L.; Theron, A.; Zussman, E. *J. Fluid Mech.* **2004**, *516*, 349−377.
(33) Lee, T. H.; Wang, J.; Wang, C.-H. *J. Controlled Release* **2002**, *83*, 437−452.
(34) Rao, J. K.; Rao, K. P. *J. Bioact. Compat. Polym.* **1997**, *12*, 127−139.
(35) Jalil, R.; Nixon, J. *J. Microencapsulation* **1990**, *7*, 297−325.
(36) Baker, R. *Controlled Release of Biologically Active Agents*; John Wiley & Sons: New York, 1987.
(37) Ctierke, T. D.; Hsu, W. Y. *The Cluster-Network of Ion Clustering in Perfluorosulfonated Membranes*; ACS Symposium Series 180; American Chemical Society: Washington, DC, 1982.
(38) Wheeler, R. G.; Friel, P. G. In *Controlled Release of Pesticides and Pharmaceuticals*; Lewis, D. H., Ed.; Plenum: New York, 1981.
(39) Moore, G. A. Connectivity of Dispersed Particles: A Probabilistic Computation. In *Proceedings of the Fourth International Congress for Stereology*; Gaithersburg, MD, Sept. 4−9, 1976.
(40) Zhang, Y. Z.; Feng, Y.; Huang, Z. M.; Lim, C. T.; Ramakrishna, S. *Nanotechnology* **2006**, *17*, 901−908.
(41) Zhang, X.; Wyss, U. P.; Pichora, D.; Amsden, B.; Goosen, M. F. A. *J. Controlled Release* **1993**, *25*, 61−69.
(42) Cleek, R. L.; Ting, K. C.; G. Eskin, S.; Mikos, A. G. *J. Controlled Release* **1997**, *48*, 259−268.
(43) Park, T. G.; Cohen, S.; Langer, R. *Pharm. Res.* **1992**, *9*, 37−39.
(44) Jiang, H.; Fang, D.; Hsiao, B. S.; Chu, B.; Chen, W. *Biomacromolecules* **2004**, *5*, 326−333.
(45) Jia, H.; Zhu, G.; Vugrinovich, B.; Kataphinan, W.; Reneker, D.; Wang, P. *Biotechnol. Prog.* **2002**, *18*, 1027−1032.

BM050743I